

# Double-Differential Neutron Emission Cross Sections on $^{209}\text{Bi}$ at 14.1 MeV Incident Energy

T Vilaithong, U Tippawan, S Singkarat and S Wiboolsake

Fast Neutron Research Facility, Department of Physics, Faculty of Science, Chiang Mai University, Chiang Mai 50200, Thailand.

Received 6 Feb 1999

**ABSTRACT** The energy and angular distributions of neutrons above 3 MeV emitted from collisions of 14.1 MeV neutrons with bismuth target were measured using the high resolution time-of-flight (TOF) facility at Chiang Mai University. The results are compared with the most recent measurements and with the calculated spectra based on the statistical multistep model code EXIFON. The angular distributions of the secondary neutrons were analyzed by the Kalbach-Mann systematics using the more recent coefficients of Kumabe *et al.* In the case of bismuth, the measured and calculated spectra only agree in the limited energy region between 6 and 12 MeV.

**KEYWORDS:** nuclear reaction,  $^{209}\text{Bi}$  (n,xn'), E=14.1 MeV, statistical multistep theory analysis.

## INTRODUCTION

Analysis of neutron emission cross sections for vibrational nuclei in terms of quantum mechanical, statistical multistep reaction mechanisms have been complicated because of interference from neutrons resulting from collective excitations. Attempts have been made to include these contributions. Kalka *et al.*<sup>1</sup> considered only those collective excitations to the lowest  $2^+$  and  $3^-$  states. Marcinkowski *et al.*<sup>2</sup> and Demetriou *et al.*<sup>3</sup> include the direct reactions that excite isoscalar, low-energy vibrations as well as the giant resonance in the continuum in their analysis. They compared their calculated results with the high resolution measurements of Takahashi *et al.*<sup>4</sup> The calculated and measured spectra do not agree over the entire energy region. We report here the measurements and analysis of these spectra for bismuth. The closed shell nucleus  $^{209}\text{Bi}$  has been one of the few elements proposed as a candidate for a neutron multiplier in the conceptual design of fusion reactor.<sup>5</sup> Therefore, accurate measurements of its double-differential cross sections (DDX) and angle integrated cross sections are also needed for the practical application. Apart from the experiment of Takahashi *et al.*<sup>4</sup>, there have been very few high resolution measurements of the neutron emission spectra of bismuth in the last decade. Wang *et al.*<sup>6</sup> measured the neutron emission spectra and angular distributions at 7 MeV neutron bombarding energies with 5.1 m flight path and 2 ns time resolution corresponding to 400 keV resolution for the elastically scattered neutrons. Marcinkowski *et al.*<sup>7</sup> carried out similar measurement at 20 MeV with an energy resolution of about 600 keV. The most recent

DDX measurement of bismuth was performed by Baba *et al.*<sup>8</sup> for incident neutrons of 14.1 and 18.0 MeV. The overall timing resolution of their spectrometer was 2.0 to 2.5 ns and the flight path was around 6 m for 14 MeV measurement. Therefore, only one high resolution experiment<sup>4</sup> has been performed at 14 MeV for bismuth, the measurements reported here provide an important separate determination of these spectra.

## MATERIALS AND METHODS

### Experimental Procedure

The experiment was performed at the high resolution time-of-flight (TOF) facility of the Fast Neutron Research Facility of Chiang Mai University. The production of a ns pulsed neutron beam was described in an earlier publication.<sup>9</sup> Briefly, neutrons with energy of 14.1 MeV were produced from a high stability Cockcroft-Walton-type accelerator by the  $\text{T}(d,n)^4\text{He}$  reaction. The 140 keV analysed deuteron beam was chopped by a double-plate deflecting system and then bunched by a double-gap klystron buncher to produce beam pulses with widths of 1.5 to 2.0 ns at the neutron production target. This work utilized an average beam of about 15 mA with a neutron pulsed width of about 1.8 ns at 1 MHz repetition rate.

The experimental arrangement and data reduction procedure used in the present measurement were similar to those described previously.<sup>10</sup> A schematic diagram of the experimental set up is shown in Fig 1. A cylindrical sample of  $^{209}\text{Bi}$ , 3 cm in diameter and 7 cm long, was positioned at  $90^\circ$  relative to the incident deuteron beam with its axis along the axis

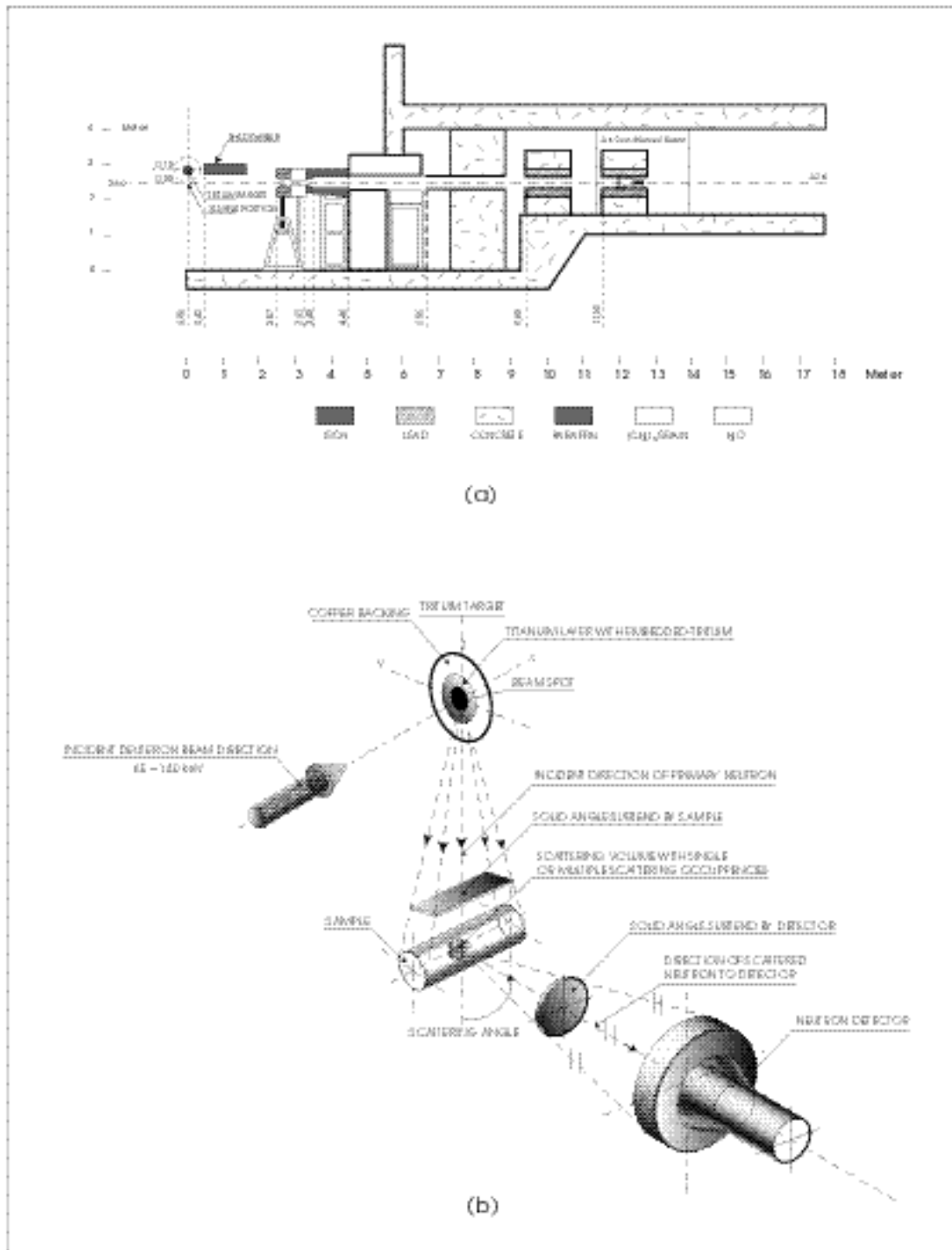


Fig 1. Experimental arrangement for the TOF measurement (a) collimating and shielding arrangement (b) target arrangement.

of the beam line. The target was cooled by forced air. A sample rotation technique provides the capability of measuring scattered neutrons over an angular range of  $20^\circ$  to  $160^\circ$ .

The scattered neutrons were detected with a 25.0 cm diam and 10.0 cm thick BC-501A liquid scintillator. The detector was coupled to a Hamamatsu R1250 photomultiplier tube via a partially coated taper light pipe. It was located at an extended flight path of 12 m inside a well shielded tunnel as shown in Fig 1. Monte Carlo calculation indicates that effect due to in-scattered neutrons is less than 1%.<sup>11</sup> The neutron detector was housed in a temperature controlled room to minimize photomultiplier tube gain drift. Neutron fluxes were monitored by three 5 cm diam by 5 cm thick NE-102A and NE-213 scintillators. This flux monitoring system is accurate to better than 1%.

The electronic system used in this measurement has been described in details elsewhere.<sup>10</sup> Only a brief description will be given here. A pulse-shape discrimination system (PSD) based on a zero-cross over method was incorporated into the main electronic system to reduce the gamma-ray background. The data acquisition system is controlled by a 16MB MicroVAXII computer through a multiparameter-buffer system (MBS) unit. Each reaction event detected by the main detector is recorded sequentially in list mode on disk. Each event contains (i) the pulse height, (ii) the time-of-flight, and (iii) the n-gamma pulse shape discrimination data. The off line analysis software allows dynamic selection for each correlated parameter.

Calibration of the pulse height response of the main detector was performed in about 8 h intervals before and after each scattering angle with  $^{137}\text{Cs}$  and  $^{22}\text{Na}$  gamma sources. The pulse height threshold was set at about 1.5 MeV proton energy. At this bias setting, the corresponding energy resolution of our neutron spectrometer at 14.1 MeV was about 420 keV FWHM. Time-of-flight spectra were obtained at 14 angles between  $20^\circ$  to  $150^\circ$  in  $10^\circ$  increment. For each set of measurement, a "sample-in" spectrum was taken followed by a "sample-out" spectrum. A polyethylene sample of the same dimension as that of the bismuth sample was used as standard and positioned at  $25^\circ$  relative to the incident neutron beam. Each run took about 3-4 h, therefore, the measurement at one angle including the "out target" run lasted about 7-8 h. During this period the stability of the electronic system was better than 1%.

A typical TOF spectrum of bismuth at  $20^\circ$  is shown in Fig 2. The sample-out spectrum is also shown for comparison. The background spectrum is clean and no structure was observed in the region of interest. The prompt gamma ray peak was used as reference to convert TOF spectrum to energy spectrum.

#### Data reduction

Neutron energy spectra were obtained from the measured TOF spectra using the known flight path and a calibration of time-to-amplitude converter. The DDX in units of b per sr per MeV were determined using the detector efficiency, monitor counts, and  $^1\text{H}(n, n)$  cross section as standard. The neutron detecting efficiencies were calculated with the Monte

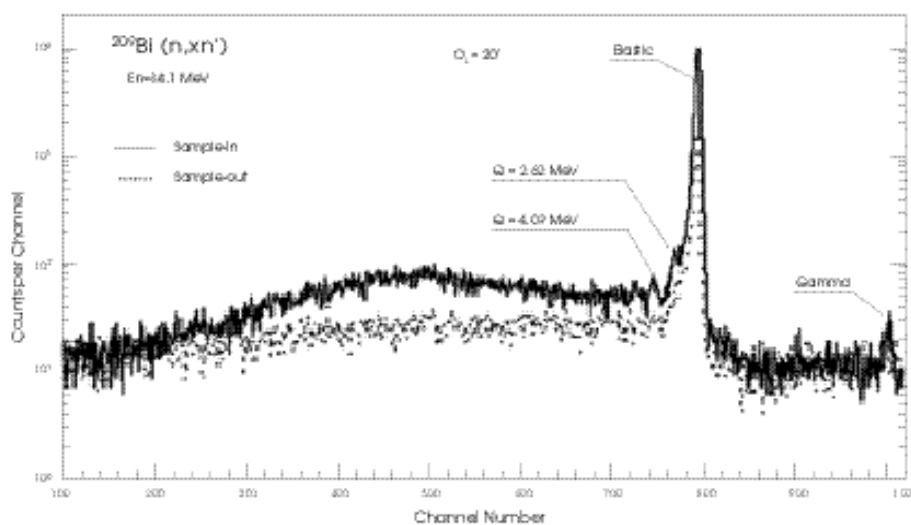


Fig 2. A typical TOF spectrum of bismuth at  $20^\circ$ . The sample-out run is shown for comparison.

Carlo computer code.<sup>12</sup> The differential cross sections were averaged over 0.2 MeV energy bin which corresponded to the energy resolution of the TOF spectrometer. The experimental procedure and data reduction is similar to that described in details elsewhere.<sup>10</sup> The correction for multiple scattering, flux attenuation and contamination of low energy neutrons in the incident neutron spectrum was performed using a Monte Carlo computer code SYNTHIA developed by Baba *et al*<sup>13</sup> at Tohoku University.

The DDX data were converted from the laboratory system to the center-of-mass system (CM), by assuming the kinematics of two body reaction.<sup>14</sup> The angle-integrated neutr on spectrum (EDX) in the CM system was obtained by weighted the angular distribution for each energy bin with experimental uncertainties and fitted with Legendre polynomials. The EDX in the CM system is used for comparison with other measurements and calculated cross sections.

The overall systematic error for the DDX is estimated to be  $\pm 11\%$ . This number was obtained from the quadratic sum of the following uncertainties: (1)  $\pm 3\%$  for the neutron detecting efficiency; (2)  $\pm 2\%$  for the variation of the incident neutron yield; (3)  $\pm 1\%$  for H cross section; (4)  $\pm 1\%$  for the monitor; (5)  $\pm 2\%$  for estimating hydrogen scattering yield; (6)  $\pm 10\%$  for the flux attenuation and multiple scattering corrections of polyethelene and bismuth samples. The experimental uncertainties were estimated by combining the statistical and systematic uncertainties in quadrature.

### Model calculations

Nuclear model calculations of 14.1 MeV neutron inelastic scattering on <sup>209</sup>Bi have been performed with the statistical multistep model code EXIFON.<sup>15</sup> This code is based on an analytical model for statistical multistep direct and multistep compound reaction (SMD/SMC). EXIFON predicts the secondary particle angular distributions in addition to their emission spectra (EDX). In this section we summarize these calculations and describe the parameters used in our calculations.

The code EXIFON calculates the overall energy differential cross section on the basis of pure quantum mechanical concept by summing up the contributions from the SMD, SMC and multiparticle emission (MPE) processes. This idea constitutes a very strong place in nuclear reaction theory as being supported by its counterpart in many body theory. The residual interactions are replaced by random matrices and after performing the energy ensemble

averaging, the analytical expressions for the energy differential cross section; (EDX) becomes<sup>15</sup>

$$\frac{d\sigma_{a,xb}(E_a)}{dE_b} = \frac{d\sigma_{a,b}^{\text{SMD}}(E_a)}{dE_b} + \frac{d\sigma_{a,b}^{\text{SMC}}(E_a)}{dE_b} + \frac{d\sigma_{a,b}^{\text{MPE}}(E_a)}{dE_b} \quad (1)$$

where the direct reaction to collective phonon and single particle states are accounted for as a part of the SMD process, and the MPE are calculated in the pure SMC concept. For our nuclide of interest, <sup>209</sup>Bi, the optical model potentials of Wilmore and Hodgson<sup>16</sup> are adopted. The only adjustable parameter is the pairing shift ( $\Delta = 12.8 A^{-1/2}$ ) which goes to zero near closed shell. The shell correction for the state density are also taken into account for the process. The present calculations are performed with a Breit-Wigner function of width 0.9 MeV instead of the built in value of 1.4 MeV to simulate the higher energy resolution in our experiments. Other parameters are left unadjusted. The effect of angular momentum and nuclear spin are not considered to make the calculation as simple as possible without any significant effects.

The ADXs are calculated using the Kalbach-Mann systematics.<sup>17</sup> These systematics give the DDX for particle emission reaction by superposing the forward peaked distribution for SMD on the 90° symmetric distribution of SMC process taking into account the weight of the SMD:

$$\frac{d^2\sigma}{d\Omega dE} = a_0(\text{SMD}) \sum_{\ell=0}^{\ell_{\text{max}}} b_{\ell} P_{\ell}(\cos\theta) + a_0(\text{SMC}) \sum_{\ell=0, \Delta\ell=2}^{\ell_{\text{max}}} b_{\ell} P_{\ell}(\cos\theta) \quad (2)$$

where 
$$b_{\ell}(E) = \frac{2\ell+1}{1 + \exp[A_{\ell}(B_{\ell} - E)]}$$

We have used the more recent coefficients of Kumabe *et al*<sup>18</sup>

$$A_{\ell} = 0.0561 + 0.0377\ell \text{ MeV}^{-1}$$

$$B_{\ell} = 47.9 - 27.1\ell^{-1/2} \text{ MeV}$$

The coefficients  $a_0$  in (2) satisfy the relation

$$a_0(\text{total}) = a_0(\text{SMD}) + a_0(\text{SMC}) \quad (3)$$

$a_0(\text{SMD})$  and  $a_0(\text{SMC})$  are obtained from EXIFON taking account of direct (DR) and MPE components in multistep direct (SMD) and multistep compound (SMC) respectively.

## RESULTS AND DISCUSSION

### Comparison with other measurements

The double-differential cross sections obtained in our measurement for bismuth are shown in Fig. 3 and they are available in tabular form upon request. The angle-integrated cross sections (EDX) are presented in Table 1. In Fig 4, we compare our measurements at 30° and 120° with those of Takahashi *et al*<sup>4</sup> and Baba *et al*<sup>8</sup>. The error bars shown on our data are statistical only. The three different sets of measurements are in general agreement to within 10 to 20%. Nevertheless, our data reveals more detailed structures in the region between 6 to 12 MeV which is due to direct excitation of low-lying vibrational levels. It should be noted that Takahashi *et al*<sup>4</sup> used 8.3 m flight path for his TOF measurement so his energy resolution is almost comparable to ours whereas Baba *et al*<sup>8</sup> measured their neutron spectra with poorer energy resolution. Fig 5 illustrates the angle-integrated cross sections of Bi from three different experiments. The effect due to difference in the energy resolution of the TOF

spectrometer can be clearly observed in the spectral regions where broad peaks are located. The enhancement of these structures in <sup>209</sup>Bi is to be expected because it is next to the double-closed-shell <sup>208</sup>Pb.

### Theoretical analysis

### Angle-integrated neutron emission cross section (EDX)

The nuclear model calculations described under the heading model calculations have been performed and the results compared to the experimental data. The calculated spectrum is presented together with

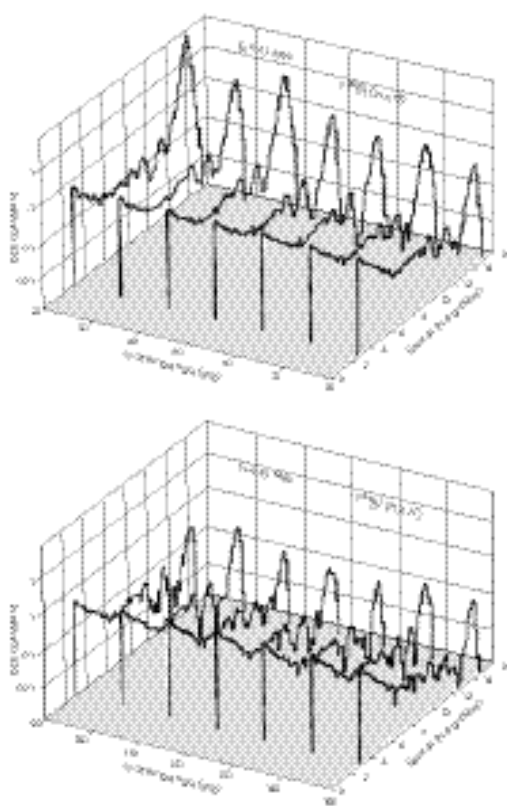


Fig 3. Double-differential cross sections of <sup>209</sup>Bi from 20° to 150° in step of 10° at 14.1 MeV in the laboratory system.

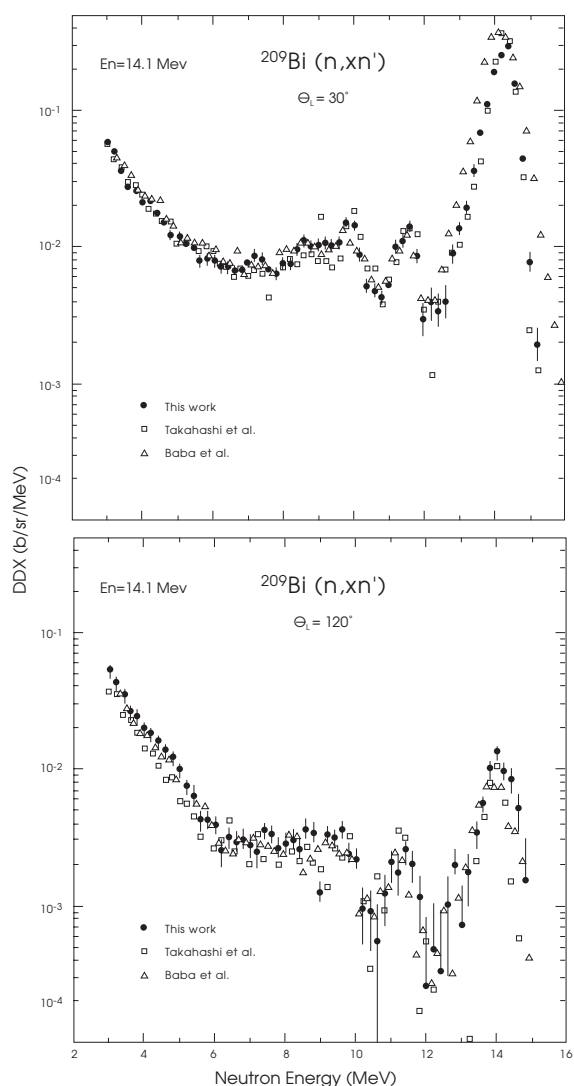


Fig 4. Double-differential cross sections of <sup>209</sup>Bi at (a) 30° and (b) 120°. The data of Takahashi *et al*<sup>4</sup> and Baba *et al*<sup>8</sup> are shown for comparison.

**Table 1.** Angle-integrated cross-sections of  $^{209}\text{Bi}$  in the CM system. The errors shown are experimental uncertainties.

Energy (MeV)	EDX (b/MeV)	Energy (MeV)	EDX(b/MeV)
3.0	6.45±0.74E-1	9.2	5.31±0.89E-2
3.2	5.35±0.62E-1	9.4	5.49±0.90E-2
3.4	4.32±0.51E-1	9.6	7.30±1.12E-2
3.6	3.59±0.43E-1	9.8	8.38±1.26E-2
3.8	3.03±0.37E-1	10.0	6.89±1.09E-2
4.0	2.60±0.32E-1	10.2	4.11±0.75E-2
4.2	2.26±0.28E-1	10.4	2.67±0.56E-2
4.4	1.94±0.25E-1	10.6	2.14±0.48E-2
4.6	1.66±0.22E-1	10.8	2.62±0.56E-2
4.8	1.51±0.20E-1	11.0	3.25±0.63E-2
5.0	1.32±0.18E-1	11.2	5.30±0.88E-2
5.2	1.14±0.16E-1	11.4	7.49±1.14E-2
5.4	9.24±1.36E-2	11.6	6.97±1.09E-2
5.6	7.61±1.17E-2	11.8	3.65±0.70E-2
5.8	7.24±1.12E-2	12.0	1.99±0.50E-2
6.0	6.93±1.09E-2	12.2	1.84±0.47E-2
6.2	5.71±0.94E-2	12.4	2.29±0.52E-2
6.4	5.05±0.86E-2	12.6	3.05±0.60E-2
6.6	5.28±0.89E-2	12.8	4.41±0.77E-2
6.8	4.99±0.85E-2	13.0	6.60±1.01E-2
7.0	5.04±0.85E-2	13.2	1.15±0.16E-1
7.2	5.40±0.90E-2	13.4	2.51±0.30E-1
7.4	5.43±0.90E-2	13.6	5.32±0.61E-1
7.6	5.28±0.89E-2	13.8	9.58±1.07E-1
7.8	5.28±0.89E-2	14.0	1.22±0.14E-0
8.0	5.54±0.94E-2	14.2	9.81±1.10E-1
8.2	5.81±0.96E-2	14.4	5.53±0.65E-1
8.4	6.36±1.02E-2	14.6	2.29±0.29E-1
8.6	6.79±1.07E-2	14.8	6.74±1.19E-2
8.8	6.63±1.06E-2	15.0	3.87±0.96E-2
9.0	5.64±0.94E-2	15.2	2.35±0.73E-2

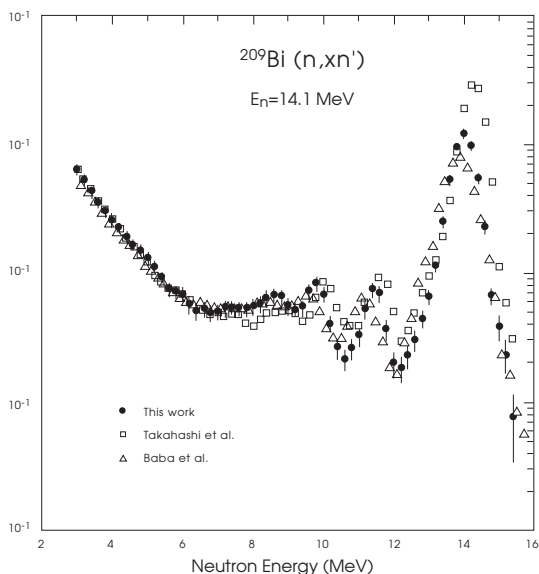


Fig 5. Angle-integrated spectra of  $^{209}\text{Bi}$  in the CM system. The error bars are derived from experimental uncertainties.

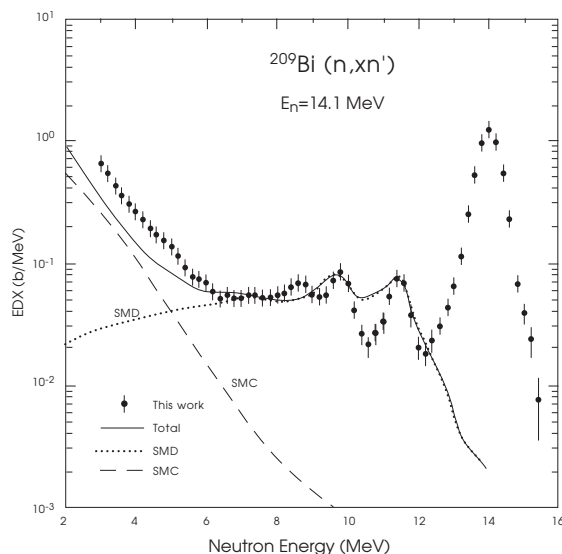


Fig 6. Comparison of the angle-integrated spectrum with the calculation by EXIFON.

the measured spectrum in Fig 6. For the sake of comparison, the separate contributions from SMD and SMC are also shown in the figure. On the whole, the neutron production spectrum in the continuum between 3 – 5 MeV (low emission energy region, or high excitation energies of the residual nucleus) is underestimated by the model calculation by about 30%. As the measurement has relatively small uncertainties, some deviation between calculations and experiments are clearly noticed. At about 5 – 8 MeV, the calculations reproduce the data very well. In the energy region between 8 to 11 MeV when only two excited levels  $2^+$  and  $3^-$  are considered, the shapes and structures of the measured spectrum are poorly reproduced by the calculation. But when all nine excited levels ( $2^+$ ,  $3^-$ ,  $4^+$ ,  $5^-$ ,  $6^+$ ,  $7^-$ ,  $8^+$ ,  $9^-$ ,  $10^+$ ) are incorporated, the calculated result reproduces the experimental data fairly well apart from the bump at 10 MeV, which is to be expected as the calculated spectrum is smeared out using a Gaussian resolution function normalized to the gamma width. The values of the deformation parameter,  $\beta_1$ , and the energies,  $E_{x^i}$ , of the collective excited low-lying states are taken from those of  $^{208}\text{Pb}$ .<sup>3</sup> The result confirms that in this energy region, the collective excitations to low-lying states play important role. However, the code also takes only the lowest energy state of each level as an input for calculations. This may as well be the cause of the remaining discrepancy between the calculated and measured spectra in this energy region.

Changing the values of model parameters does not significantly improve the calculated results. Since all the energy levels are taken from those of  $^{208}\text{Pb}$ , the double magic nuclei, the difficulty discussed by Marcinkowski *et al*<sup>7</sup> may be relevant here.

In summary, our calculation largely underestimates the present measured EDX data for  $^{209}\text{Bi}$  in the continuum region. The shape and structures of the measured spectrum are fairly reproduced in the region where collective excitation of low-lying states are important. The discrepancies in the yield and structure reproduction, as a result of taking only the  $2^+$  and  $3^-$  levels into consideration, are also reported by Baba *et al*.<sup>13</sup>

**Angular distribution (ADX)**

Fig 7 a) to d) compare the measured ADX at fixed energy of 3-4, 5-6, 6-7 and 8-9 MeV with the calculated ADXs obtained from Kalbach-Mann systematics<sup>17</sup> with the new coefficient of Kumabe *et al*.<sup>18</sup> The shape of the calculated angular distributions are in good agreement with those of the measured ones, although the magnitudes are slightly underestimated. The DR and MPE components have been included into SMD and SMC, respectively.

To summarize, Kalbach-Mann systematics with the new coefficients from Kumabe *et al*<sup>18</sup> reproduce quite satisfactorily the neutron ADX for  $^{209}\text{Bi}$  using the SMD and SMC spectra for  $a_0(\text{SMD})$  and  $a_0(\text{SMC})$ .

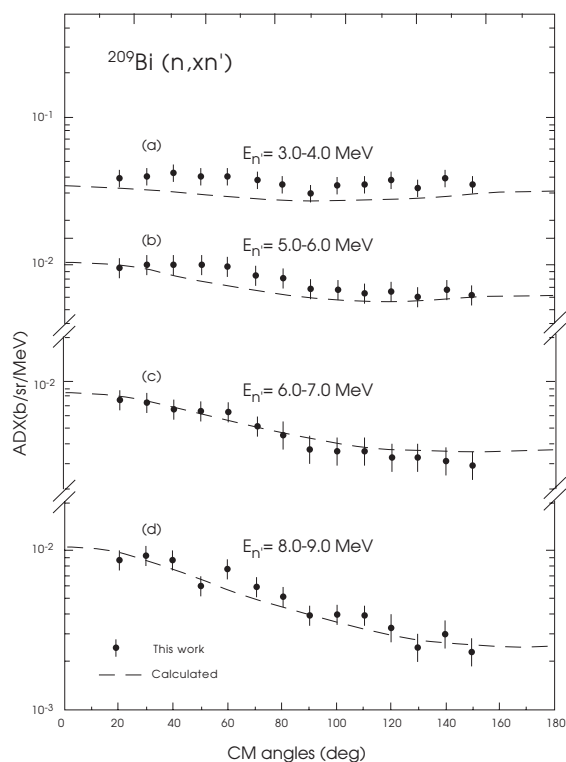


Fig 7. Comparison of the ADXs with the calculated distributions using Kalbach-Mann systematics.

## CONCLUSIONS

We measured the double differential neutron emission cross sections of  $^{209}\text{Bi}$  induced by 14.1 MeV neutrons with a high resolution time-of-flight spectrometer. The measured spectra are in reasonable agreement with the other high resolution measurements and reveals structures in the region between 8 to 12 MeV. The calculated spectrum based on the statistical multistep model code EXIFON reproduces the experimental data fairly well in the limited energy range between 6 and 12 MeV. The code underestimates the neutron yield in the compound nucleus region by as much as 30%. The shape of the angular distribution is reproduced reasonably well by the systematics of Kalbach Mann using coefficients of Kumabe *et al.* For better reproduction of neutron yields and structures in the measured spectra further theoretical studies are required.

## ACKNOWLEDGEMENTS

We are grateful to A Takahashi for providing the bismuth sample and M Baba for the SYNTHIA computer code. We thank F Maekawa for the latest version of the Japanese evaluated nuclear data library and helpful discussions. The technical support of S Rattananin in running the pulsed neutron generator and M Rhode in maintaining the data acquisition system are gratefully acknowledged. This work was supported in part by the Thailand Research Fund.

## REFERENCES

1. H Kalka, M Torjman and D Seelinger (1989) *Phys Rev C* **40**, 1619.
2. A Marcinkowski, B Marianski, P Demetriou and PE Hodgson, (1995) *Phys Rev C* **52**, 2021.
3. P Demetriou, A Marcinkowski and PE Hodgson (1996) *Nucl Phys A* **529**, 67.
4. A Takahashi, M Gotoh, Y Sasaki and H Sugimoto (1992) OKTAVIAN Report A-92-01, Osaka University.
5. ET Cheng (1986) *Proc IAEA Advisory Group Meeting on Nuclear Data for Fusion Reactor Technology*, Dresden.
6. X Wang, Y Wang, D Wang and J Rapaport, (1987) *Nucl Phys A* **465**, 483.
7. A Marcinkowski, J Rapaport, R Finlay and X Aslanoglou, (1991) *Nucl Phys A* **530**, 75.
8. M Baba, S Matsuyama, T Ito, T Ohkubo and N Hirakawa (1994) *J Nucl Sci Technol* **31**, 757.
9. T Vilaithong, S Singkarat, W Pairsuwan, JF Kral, D Boonyawan, D Suwannakachorn, S Konklong, P Kanjanarat and GG Hoyes (1991) *A Pulsed Neutron TOF Facility at Chiang Mai*. In: *Proc Int Conf Nuclear Data for Science and Technology*, Juelich, 1991, SM Qaim (Ed) Springer-Verlag, pp 482-6.
10. T Vilaithong, D Boonyawan, S Konklong, W Pairsuwan and S Singkarat (1993) *Nucl Instr and Meth A* **332**, 561.
11. H Kobus, T Vilaithong, W Pairsuwan and S Singkarat (1994) *Monte Carlo Simulation on the Neutron Transport of the Chiang Mai TOF-Facility*. In: *Proc Int Conf on Nuclear Data for Science and Technology*, Gatlinburg, 1994, JK Dickens (Ed) pp111-4.
12. R Cecil, BD Anderson and R Madey (1979) *Nucl Instr and Meth* **161**, 439.
13. M Baba, S Matsuyama, M Ishikawa, S Chiba, T Sakase, H Hirakawa (1995) *Nucl Instr and Meth A* **366**, 354.
14. A Takahashi, Y Sasaki and H Sugimoto (1988) Report JAERI-M-88-065, p 279.
15. H Kalka (1991) *Code EXIFON* (version 2.0).
16. D Wilmore and PE Hodgson (1964) *Nucl Phys* **55**, 673.
17. C Kalbach and FM Mann (1981) *Phys Rev C* **23**, 112.
18. I Kumabe, Y Watanabe, Y Nohtomi, M Hanada (1990) *Nucl Sci Eng* **104**, 280.